

Detection of Ga suboxides and their impact on III-V passivation and Fermi-level pinning

C. L. Hinkle,^{1,2,a)} M. Milojevic,¹ B. Brennan,³ A. M. Sonnet,² F. S. Aguirre-Tostado,¹ G. J. Hughes,³ E. M. Vogel,^{1,2,b)} and R. M. Wallace^{1,c)}

¹Department of Materials Science and Engineering, The University of Texas at Dallas, Richardson, Texas 75080, USA

²Department of Electrical Engineering, The University of Texas at Dallas, Richardson, Texas 75080, USA

³School of Physical Sciences, Dublin City University, Glasnevin, Dublin 9, Ireland

(Received 29 January 2009; accepted 27 March 2009; published online 20 April 2009)

The passivation of interface states remains an important problem for III-V based semiconductor devices. The role of the most stable bound native oxides GaO_x ($0.5 \leq x \leq 1.5$) is of particular interest. Using monochromatic x-ray photoelectron spectroscopy in conjunction with controlled GaAs(100) and InGaAs(100) surfaces, a stable suboxide (Ga_2O) bond is detected at the interface but does not appear to be detrimental to device characteristics. In contrast, the removal of the Ga 3+ oxidation state (Ga_2O_3) is shown to result in the reduction of frequency dispersion in capacitors and greatly improved performance in III-V based devices. © 2009 American Institute of Physics. [DOI: 10.1063/1.3120546]

The viability of field effect electronic devices made of III-V compound semiconductors has long been hindered by the presence of defects at the interface between the semiconductor and gate insulator. Despite having been studied in great detail for more than 35 years, this interface and the identification of the bonding configurations that cause the defects has remained challenging.¹⁻⁴ Problems with metal-oxide-semiconductor (MOS) devices on GaAs and InGaAs, including frequency dispersion of capacitance and suboptimal electron mobility, have been attributed to a number of different surface species including Ga–O bonds, As–O bonds, elemental As, and As and Ga antisites.⁵ Recent studies have shown that Ga–O (Ref. 6) may be the most important of these species to control, and previous research has suggested that the deposition of a specific Ga suboxide may be necessary for a low defect density.^{7,8} The determination of the specific bonding configurations that give rise to these interfacial trap defects has great implications for the electronics industry in the move away from Si-channel devices to those with higher mobility, such as GaAs and InGaAs.

The accurate identification of the oxidation states of Ga is often thought to be limited to high photon intensity synchrotron x-ray photoelectron spectroscopy (XPS) data and is usually only applied to the Ga 3*d* spectrum. The study of this spectrum with typical laboratory-based x-ray sources results in energetic photoelectrons [kinetic energy (KE) ≈ 1465 eV for an Al *K* α x-ray source] resulting in a significant decrease in sensitivity to photoelectrons originating from the near surface region. In contrast, the Ga 2*p* spectrum (KE ≈ 369 eV) exhibits considerable surface sensitivity but is notoriously difficult to deconvolve into individual oxidation states due to the broad Gaussian widths of the peaks in conjunction with the proximity of the chemical state peak positions. Moreover, the Ga 2*p* extreme surface sensitivity makes *ex situ* studies difficult due to the ultrathin films nec-

essary for photoelectron transparency and the susceptibility of the film to spurious contamination and oxidation. However, the identification of these bonding states is crucial in terms of the relation to potential defects at the interface with the III-V semiconductor.

By using numerous surface cleans, treatments, and *in situ* deposition and analysis techniques to carefully control the interfacial chemical bonding, we have conclusively identified three Ga oxidation states as well as a Ga–Si bond binding energy (BE). The control, afforded by utilizing an *in situ* ultrahigh vacuum environment, in this work avoids exposure to spurious contaminants such as C, O₂, or H₂O and from exposure to the atmosphere, and therefore an accurate peak position and width for the Ga–O and Ga–Si bonding arrangements are obtained. Four reference surfaces (controls) were produced with these surface treatments in order to manipulate the elemental species at the interface and have allowed for an extremely accurate investigation of the peak binding energy positions and intensities corresponding to specific bonds. A correlation of these specific oxidation states to the interfacial defects has been determined by electrical characterization and improved device characteristics are demonstrated through the control of specific oxidation states.

The first control sample studied was a commercially grown, As-capped, molecular beam epitaxy (MBE) deposited InGaAs substrate. After removing the As capping layer with a thermal desorption technique,⁹ an atomically ordered As-rich $c(2 \times 4)$ surface reconstruction with surface O and C below detection limits was obtained. With a surface that contains only known elements associated with the substrate itself, this reference surface gives an accurate bulk Ga–As peak fit of the spectra using a single peak [Fig. 1(a)]. The fitting values for this peak (BE and width) are used as the bulk parameters in the subsequent deconvolution of the Ga 2*p* spectra from more complex interfaces originating from multiple treatments and depositions. Any deviation of the spectra from the peak values determined from this decapped sample is therefore assumed to be indicative of additional

^{a)}Electronic mail: chris.hinkle@utdallas.edu.

^{b)}Electronic mail: eric.vogel@utdallas.edu.

^{c)}Electronic mail: rmwallace@utdallas.edu.

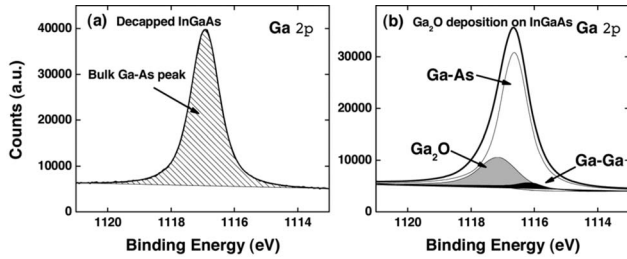


FIG. 1. (a) Ga 2*p* XPS spectrum for an As capped $\text{In}_{0.53}\text{Ga}_{0.47}\text{As}$ substrate following thermal desorption of the As cap. An oxygen and carbon free surface is produced allowing precise measurement of the position (1116.7 eV) and FWHM of the bulk peak. All XPS fits included a Shirley background subtraction. (b) Ga 2*p* XPS spectrum of an $\text{In}_{0.53}\text{Ga}_{0.47}\text{As}$ substrate following decapping and Ga_2O deposition.

bonding species other than that originating from the III-V substrate.

The next control sample was produced by directly depositing Ga_2O (Ref. 10) onto a decapped InGaAs surface. This deposition occurs through the decomposition of a Ga_2O_3 source that sublimates into Ga_2O and O_2 .⁹ The O_2 has an extremely low sticking coefficient and does not participate in surface reactions while the Ga_2O is deposited onto the III-V surface. The Ga 2*p* spectrum after this deposition reveals the BE position of a bulk Ga_2O film (seen as a shoulder on the Ga-As peak) to be at 0.55 eV above the bulk peak [Fig. 1(b)]. The Ga_2O bonding arrangement corresponds to the Ga 1+ oxidation state. The utilization of a Ga_2O_3 powder to deposit Ga_2O (rather than polycrystalline Ga_2O_3) results in the creation of Ga-Ga bonds as well [Fig. 1(b)],¹¹ making this source unacceptable for device fabrication but well suited for the spectroscopic determination of these bond peak parameters.

Higher oxidation states are seen on $\text{In}_x\text{Ga}_{(1-x)}\text{As}$ surfaces exposed to chemical treatments or atomic layer depositions (ALDs). Ga-O bonds are known to exist in chemical states that manifest themselves with binding energies around 1–2 eV above the bulk Ga-As peak.^{12–14} Treating a native oxide with NH_4OH leaves a surface oxide that exhibits a large shoulder on the high binding energy side of the bulk peak.¹⁵ The accurate analysis of this spectrum requires two oxidation states of Ga, the Ga 1+ oxidation state (Ga_2O) and the Ga 3+ oxidation state (Ga_2O_3), as shown in Fig. 2(a). Using the previously determined parameters for the bulk peak and the Ga_2O surface oxide, the precise peak position for the Ga 3+ oxidation state is determined and is found to be 1.2 eV above the bulk peak, precisely where photoelectron stud-

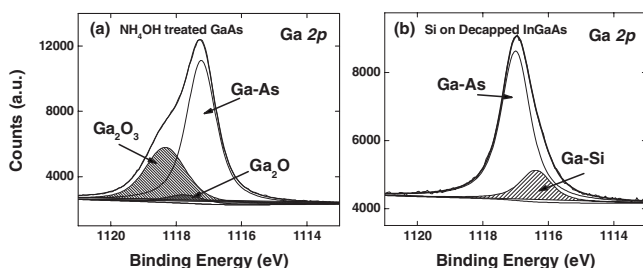


FIG. 2. (a) Ga 2*p* XPS spectrum for a NH_4OH treated GaAs substrate highlighting the location of the Ga 3+ (Ga_2O_3) oxidation state. A small interfacial Ga_2O surface oxide is also present. (b) Ga 2*p* core-level XPS spectrum of an $\text{In}_{0.53}\text{Ga}_{0.47}\text{As}$ substrate following decapping and e-beam evaporation of amorphous Si.

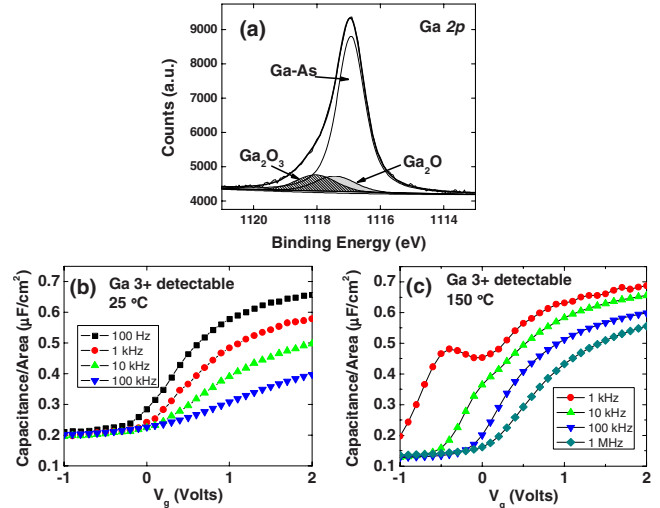


FIG. 3. (Color online) (a) Ga 2*p* XPS spectrum of ~ 1.0 nm ALD Al_2O_3 deposited on a HF-last treated GaAs surface. The presence of Ga 3+ and Ga 1+ oxidation states are both detected. (b) C-V curves from devices with the same interface as the sample from (a). (c) C-V measurements performed at 150 °C (100 Hz curves were removed due to equipment-induced noise).

ies of Ga_2O_3 powders place it. There is also a higher binding energy state that is sometimes seen in the Ga 2*p* spectra, which arise at 1.6 eV above the bulk peak and is seen only on samples with relatively thick oxides. Possible identities for this oxidation state (which was not studied here) include $\text{Ga}(\text{AsO}_3)_3$ (Ref. 12) as well as $\text{Ga}(\text{OH})_3$. This state is removed easily with chemical treatment. In contrast to previous studies, we do not detect the presence of GaO (Ga 2+) nor is it necessary to gradually broaden the width of the sequential oxidation states.¹⁶

A Si “passivation layer” is often used to improve the electrical characteristics of III-V MOS devices.¹⁷ It is therefore necessary to determine the presence and parameters of Ga-Si bonds to ensure accurate analysis of the Ga 2*p* spectrum. Hence, a control sample was made by e-beam evaporation of amorphous Si *in situ* onto the decapped InGaAs surface.⁹ The Ga 2*p* spectrum for this sample [Fig. 2(b)] is shown to have a shoulder at binding energies below that of the bulk Ga-As peak. This spectrum can be deconvolved into two peaks: the bulk Ga-As (with parameters used from the earlier decapped reference sample) and a peak 0.69 eV below the Ga-As bulk peak attributed to Ga-Si bonding. Using the peak positions of the Ga-Si bond as well as the three oxidation states accurately fits all the spectra from more than the 15 different surface treatments studied here.

Examination of the Ga 1+ oxidation state that arises after chemical treatments or depositions reveals that it is an interfacial bond of 1 ML or less coverage and its presence is always detected any time there is detectable surface oxygen. This surface concentration makes this oxidation state of utmost importance for MOS devices since any defects related to it will have direct consequences to electron transport. It has previously been suggested that Ga_2O deposition at the interface is necessary for a low defect density.^{7,8} This is direct spectroscopic evidence of its presence at the III-V interface.

The GaAs C-V curves shown in Figs. 3 and 4 correspond to capacitors with and without the Ga 3+ oxidation state as seen in the XPS spectra associated with the devices. The

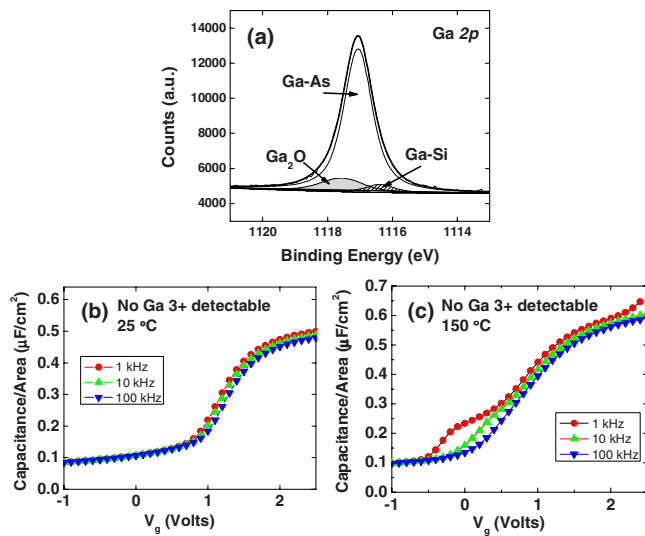


FIG. 4. (Color online) (a) Ga 2p XPS spectrum of HF-last GaAs with ~ 1.2 nm *ex situ* deposited PECVD amorphous Si followed by ~ 1.0 nm ALD Al₂O₃ deposition. The Si deposition removes the Ga 3+ oxidation state while the Ga 1+ oxidation state remains. (b) *C-V* curves from devices with the same interface as the sample from (a). (c) *C-V* measurements performed at 150 °C. The frequency dispersion has been greatly reduced, demonstrating the correlation between the Ga 3+ oxidation state and interface traps that pin the Fermi level for these systems.

Ga 3+ oxidation state is present for the device with a 10 nm Al₂O₃ directly deposited on a HF-treated GaAs(100) surface [Fig. 3(a)]. The resultant 25 °C *C-V* curve for a device with this interface [Fig. 3(b)] shows a large amount of frequency dispersion indicative of a high interfacial defect density and Fermi-level pinning.¹⁸ *C-V* performed at 150 °C (Ref. 19) [Fig. 3(c)] shows further evidence of this extremely high D_{it} when Ga 3+ is present at the interface. The spectrum in Fig. 4(a) shows the removal of the Ga 3+ oxidation state via *ex situ* deposited plasma enhanced chemical vapor deposition (PECVD) amorphous Si. This Si layer getters oxygen from the Ga 3+ species⁶ and also provides a barrier to further interface oxidation from subsequent processing including Al₂O₃ deposition. The 25 °C *C-V* curve for the corresponding device [Fig. 4(b)] shows a substantial reduction of frequency dispersion. The 150 °C *C-V* measurement of these devices [Fig. 4(c)] confirms a drastic reduction in D_{it} via the removal of the Ga 3+ oxidation state although this interface is still not defect free. MOS transistors using these analogous InGaAs interfaces reveal much higher drive current and transconductance from the devices in which all detectable Ga 3+ were removed.²⁰ The extracted mobility further confirms the device performance increase via the removal of Ga₂O₃ (Ref. 21). We propose that the higher oxidation states of Ga are related to the species that cause high D_{it} , and hence Fermi-level pinning either from a direct removal of defect states from Ga 3+ or from a resultant bonding reconfiguration, such as the formation of undimerized As when Ga₂O₃ is present.⁷ We again note that the Ga₂O bonding arrangement remains for *all* of these interfaces suggesting that it is not the

species primarily responsible for Fermi-level pinning. The role of the Ga-Si bond detected in the device stack (Fig. 4) and interface state redistribution remains to be investigated.²²

The authors thank Dr. M. Passlack, Professor K. J. Cho, and Professor J. Kim for their valuable discussions. This work is partially supported by the FCRP Materials Structures and Devices (MSD) Center, the Science Foundation Ireland, the System IC 2010 Program funded by COSAR (MKE), Korea, and the National Institute of Standards and Technology, Semiconductor Electronics Division. Dr. Aguirre-Tostado is now with Centro de Investigación en Materiales Avanzados, S.C., Apodaca, N.L., México 66600.

¹Physics and Chemistry of III-V Compound Semiconductor Interfaces, edited by C. W. Wilmsen (Plenum, New York, 1985).

²T. Sawada and H. Hasegawa, *Electron. Lett.* **12**, 471 (1976).

³A. Callegari, P. D. Hoh, D. A. Buchanan, and D. Lacey, *Appl. Phys. Lett.* **54**, 332 (1989).

⁴M. Passlack, M. Hong, and J. P. Mannaerts, *Appl. Phys. Lett.* **68**, 1099 (1996).

⁵W. E. Spicer, N. Newman, C. J. Spindt, Z. Lilientalweber, and E. R. Weber, *J. Vac. Sci. Technol. A* **8**, 2084 (1990).

⁶C. L. Hinkle, A. M. Sonnet, E. M. Vogel, S. McDonnell, G. J. Hughes, M. Milojevic, B. Lee, F. S. Aguirre-Tostado, K. J. Choi, J. Kim, and R. M. Wallace, *Appl. Phys. Lett.* **91**, 163512 (2007).

⁷M. J. Hale, S. I. Yi, J. Z. Sexton, A. C. Kummel, and M. Passlack, *J. Chem. Phys.* **119**, 6719 (2003).

⁸R. J. W. Hill, D. A. J. Moran, L. Xu, Z. Haiping, D. Macintyre, S. Thoms, A. Asenov, P. Zurcher, K. Rajagopalan, J. Abrokwhah, R. Droopad, M. Passlack, and I. G. Thayne, *IEEE Electron Device Lett.* **28**, 1080 (2007).

⁹Detailed descriptions of experimental methods are discussed in C. L. Hinkle, M. Milojevic, A. M. Sonnet, H. C. Kim, J. Kim, E. M. Vogel, and R. M. Wallace, "Graphene and emerging materials for Post-CMOS applications," ECS Trans. (to be published).

¹⁰M. Passlack, in *III-V Semiconductor Heterostructures: Physics and Devices*, edited by W. Z. Cai (Transworld Research, Kerala, 2003), pp. 327–355.

¹¹Z. Yu, C. D. Overgaard, R. Droopad, M. Passlack, and J. K. Abrokwhah, *Appl. Phys. Lett.* **82**, 2978 (2003).

¹²G. Hollinger, R. Skheytakabbani, and M. Gendry, *Phys. Rev. B* **49**, 11159 (1994).

¹³G. Landgren, R. Ludeke, Y. Jugnet, J. F. Morar, and F. J. Himpsel, *J. Vac. Sci. Technol. B* **2**, 351 (1984).

¹⁴C. C. Surdu-Bob, S. O. Saied, and J. L. Sullivan, *Appl. Surf. Sci.* **183**, 126 (2001).

¹⁵M. V. Lebedev, D. Enslin, R. Hunger, T. Mayer, and W. Jaegermann, *Appl. Surf. Sci.* **229**, 226 (2004).

¹⁶J. Ivanco, T. Kubota, and H. Kobayashi, *J. Appl. Phys.* **97**, 073712 (2005).

¹⁷J. L. Freeouf, D. A. Bachanan, S. L. Wright, T. N. Jackson, and B. Robinson, *Appl. Phys. Lett.* **57**, 1919 (1990).

¹⁸C. L. Hinkle, A. M. Sonnet, M. Milojevic, F. S. Aguirre-Tostado, H. C. Kim, J. Kim, R. M. Wallace, and E. M. Vogel, *Appl. Phys. Lett.* **93**, 113506 (2008).

¹⁹G. Brammertz, H.-C. Lin, K. Martens, D. Mercier, S. Sioncke, A. Delabie, W. E. Wang, M. Caymax, M. Meuris, and M. Heyns, *Appl. Phys. Lett.* **93**, 183504 (2008).

²⁰A. M. Sonnet, C. L. Hinkle, M. N. Jivani, R. A. Chapman, G. P. Pollack, R. M. Wallace, and E. M. Vogel, *Appl. Phys. Lett.* **93**, 122109 (2008).

²¹C. L. Hinkle, A. M. Sonnet, R. A. Chapman, and E. M. Vogel, *IEEE Electron Device Lett.* **30**, 316 (2009).

²²M. Passlack, R. Droopad, Z. Yu, N. Medendorp, D. Braddock, X. W. Wang, and T. P. Ma, *IEEE Electron Device Lett.* **29**, 1181 (2008).